Arabian Journal of Chemistry (2020) 13, 8388–8394

King Saud University

Arabian Journal of Chemistry

www.ksu.edu.sa
www.sciencedirect.com

ORIGINAL ARTICLE

Facile solvothermal synthesis of highly active monoclinic scheelite $BiVO_4$ for photocatalytic degradation of methylene blue under white LED light irradiation

Minh Que Pham [a,1], Trong Minh Ngo [b,1], Vinh Huu Nguyen [c,d], Linh Xuan Nong [c,d], Dai-Viet N. Vo [c], Thuan Van Tran [c,d], Thanh-Danh Nguyen [e,f], Xuan-Thanh Bui [a,g], Trinh Duy Nguyen [c,d,*]

[a] *Faculty of Environment and Natural Resources, Ho Chi Minh City University of Technology (HCMUT), Ho Chi Minh City 700000, Vietnam*
[b] *Faculty of Chemical Technology, Ho Chi Minh City University of Food Industry, 140 LeTrong Tan, Tan Phu District, Ho Chi Minh City 700000, Viet Nam*
[c] *Center of Excellence for Green Energy and Environmental Nanomaterials (CE@GrEEN), 300A Nguyen Tat Thanh, District 4, Ho Chi Minh City 755414, Viet Nam*
[d] *NTT Hi-Tech Institute, Nguyen Tat Thanh University, 300A Nguyen Tat Thanh, District 4, Ho Chi Minh City 755414, Viet Nam*
[e] *Institute of Research and Development, Duy Tan University, Da Nang City, Viet Nam*
[f] *Institute of Chemical Technology, Vietnam Academy of Science and Technology, 1 Mac Dinh Chi Street, District 1, Ho Chi Minh City, Viet Nam*
[g] *Key Laboratory of Advanced Waste Treatment Technology, Vietnam National University Ho Chi Minh (VNU-HCM), Linh Trung ward, Thu Duc district, Ho Chi Minh City 700000, Vietnam*

Received 20 February 2020; accepted 21 May 2020
Available online 29 May 2020

KEYWORDS

Solvothermal synthesis;
monoclinic scheelite $BiVO_4$;
Photodegradation;
LED light irradiation

Abstract In this study, $BiVO_4$ was successfully synthesized via the solvothermal process using a solvent mixture of ethylene glycol and water under different synthesis conditions of temperature and pH. Physicochemical properties such as crystal phase, morphology, and optical absorption of the as-synthesized $BiVO_4$ samples were characterized by X-ray diffraction (XRD), Raman spectra, field emission scanning electron microscopy (FE-SEM), and ultraviolet–visible diffraction

* Corresponding author at: Center of Excellence for Green Energy and Environmental Nanomaterials (CE@GrEEN), 300A Nguyen Tat Thanh, District 4, Ho Chi Minh City 755414, Viet Nam.
E-mail address: ndtrinh@ntt.edu.vn (T.D. Nguyen).
[1] The authors play the same contribution.

Peer review under responsibility of King Saud University.

Production and hosting by Elsevier

https://doi.org/10.1016/j.arabjc.2020.05.029

reflection spectroscopy (UV–vis DRS). The XRD analysis showed that different synthesis conditions of temperature and pH significantly affected the growth of monoclinic $BiVO_4$ crystals oriented along (0 4 0) facets. Form SEM results, the synthesis conditions, including pH and temperature, have a great effect on the morphology of monoclinic structured $BiVO_4$. As the pH value increases in the range of 0–9 and temperature increases from 80 °C to 180 °C, the morphology of $BiVO_4$ changed from peanut-, rod-, and leaf-like shapes. The photocatalytic activities of as-synthesized $BiVO_4$ photocatalysts were evaluated by the photodegradation of methylene blue (MB) dye under irradiation of white LED light. We have found that by using appropriate synthesis conditions (the synthesis temperature of 140 °C and the synthesis pH of 7) the $BiVO_4$ exhibited high photocatalytic efficiency for MB degradation (about 82.30% after 180 min of irradiation). This result is due to the development of the $BiVO_4$ crystals oriented along (0 4 0) facets with an increase in the intensity ratio of $I_{(0\ 4\ 0)}/I_{(1\ 2\ 1)}$. The growth of $BiVO_4$ crystals oriented along (0 4 0) facets may be beneficial to enhance the photocatalytic activity of monoclinic scheelite $BiVO_4$.

1. Introduction

Concurrent rapid industrialization and population growth result in a substantial discharge of organic pollutants, causing severe environmental pollution and posing major health risks to human. Therefore, the remediation of toxic organic waste has been the focal research direction to ensure the process of sustainable development and limit the emission of environmental pollutants. In this research direction, photocatalytic techniques using semiconductor materials provide an ideal solution in terms of solar conversion and contaminant removal (Singh et al., 2020; Rajamanickam and Shanthi, 2016; Abdennouri et al., 2016). The main advantage of this technique is that organic pollutants can be converted into CO_2, water, or other non-hazardous inorganic compounds and do not cause secondary pollution (Abbasi et al., 2018; Ameta and Ameta, 2016). Recently, monoclinic bismuth vanadate-based semiconductor photocatalyst (m-$BiVO_4$) has attracted much attention from researchers due to its non-toxicity, low cost and high photocatalytic activity. m-$BiVO_4$ has narrow band-gap energy, at about 2.4 eV, allowing photocatalysis to be directly exposed to visible light (the light area occupies 45% of the solar spectrum). Besides, it has been shown that the material could achieve high photocatalytic efficiency in water separation and decomposition of pollutants (Ressnig et al., 2012; Kohtani et al., 2003). However, due to some intrinsic properties within the structure of m-$BiVO_4$, this material has some limitations, such as weak adsorption capacity, a difficulty for the electrical charge to move to the catalytic surface, and the recombination process of electron and hole pairs, thus reducing the photocatalytic activity. To improve photocatalytic activity, recent studies have shown that the surface structure of materials plays an essential role in their photocatalytic activities since photocatalytic reactions occur only when electrons and holes are created on the surface (Lim et al., 1995; Sun et al., 2009). For $BiVO_4$ photocatalyst materials, Hui-Ling Tan and colleagues showed that $BiVO_4$ synthesized with the appropriate crystal facet ratio of (0 1 0)/(1 1 0) would give superior photocatalytic activity (Tan et al., 2016).

According to previous studies, it has been shown that the method of synthesizing materials has a significant effect on morphology, particle size, specific surface and crystal structure of heterogeneous photocatalysts, which determines adsorption and photochemical activity of as-synthesized materials (Lim et al., 1995; Sun et al., 2009; Xi and Ye, 2010). Currently, m-$BiVO_4$ can be synthesized by many methods such as solvothermal method (Zhao et al., 2013), co-precipitation method (Martínez-de la Cruz and Pérez, 2010), method of using microwave (Liu et al., 2010) and solution combustion synthesis method (Chen et al., 2015). In which, the synthesis of materials by solvothermal method allows the creation of materials with many different crystal morphologies through changing synthesis parameters. In the case of synthesis of catalytic materials by the solvothermal process, kind of solvents, synthesis temperature and time are essential factors related to the formation and development of crystals.

In this study, with the aim of obtaining $BiVO_4$ with improved photochemical properties through control of crystal morphology and crystal faces, we adopted a $BiVO_4$ synthesis routine that is based on the solvothermal method, allowing for close control of the synthesis and the structure and size of $BiVO_4$ crystals. Solvents with high boiling temperature, high viscosity, polarity, and saturated vapor pressure, such as ethylene glycol (EG), were selected to synthesize $BiVO_4$. The photocatalytic activity of the resulting materials was evaluated through the photodecomposition of methylene blue (MB) under the irradiation of LED light.

2. Experimental

2.1. Materials

Bismuth(III) nitrate pentahydrate ($Bi(NO_3)_3{\cdot}5H_2O$, ≥98.0%), ammonium metavanadate (NH_4VO_3, ≥98%) were purchased from Sigma-Aldrich. Ethylene glycol ($C_2H_6O_2$, 99.0%), ethanol (CH_3CH_2OH, 99.7%) were obtained from Xilong Chemical Co., Ltd. (China). Methylene blue (MB, $C_{16}H_{18}ClN_3S$, 99%) was purchased from HiMedia Laboratories Pvt. Ltd. (India).

2.2. Solvothermal synthesis of $BiVO_4$ catalysts

The $BiVO_4$ photocatalysts with highly photocatalytic performance were synthesized by a solvothermal method using the mixture of ethylene glycol and water as the mixed solvent

under different synthesis conditions of temperature and pH values. In a typical synthesis, 4 mmol $Bi(NO_3)_3{\cdot}5H_2O$ and 4 mmol NH_4VO_3 were dissolved in 40 mL of EG and 40 mL of H_2O, respectively. These two solutions were mixed and stirred for 1 h to obtain a yellow homogeneous solution. Then, the pH of the mixed solution was adjusted to the desired value using NH_3 solution. The mixture was transferred into an autoclave and heated at a specific temperature for 3 h. After that, the resultant suspension was centrifuged at 7000 rpm for 10 min, and the obtained $BiVO_4$ powder was dried at 60 °C overnight. Finally, they were calcined at 400 °C for 3 h and denoted as BV-x-y (x is the synthesis temperature, and was chosen as 80, 120, 140, 160, and 180 °C; y is the pH values and was chosen as 0.5, 3, 7, and 9).

2.3. $BiVO_4$ catalysts characterization techniques

Physicochemical properties such as crystal phase, morphology and optical absorption of the as-synthesized $BiVO_4$ samples were characterized by X-ray Diffractometer (XRD, Bruker D8 Advance, with a Cu Kα excitation source at a scan rate of 0.030°/s in the 2-theta range of 10–50°), Raman spectra (Horiba Jobin-Yvon, with a laser beam of 633 nm in the wavenumber of 100–1000 cm^{-1}), Scanning Electron Microscope (SEM, JEOL JSM 7401F), and ultraviolet–visible (UV–vis) diffuse reflectance spectroscopy (UV–vis DRS, Shimazu UV-2450, in the range 200–800 cm^{-1}), respectively.

2.4. Photodegradation test

The photocatalytic activity of the resulting materials was evaluated based on the photocatalytic degradation of MB dye under the irradiation source as LED (six daylight Cree® Xlamp® XM-L2 LEDs; max power of 10 W and max light output of 1052 lm). The experimental process was as follows: 50 mg of catalyst was dispersed in 100 mL of MB solution (15 ppm) and stirred in the dark for 60 min. After that, the lamp was turned on to start the photocatalytic reaction. During irradiation, 3 mL of the reaction solution was withdrawn at equal intervals to investigate the change in MB concentration. This reaction solution was centrifuged at 7000 rpm for 15 min to remove the catalysts entirely. The concentration of MB was tested on an UV–Vis (Evolution 60S UV–Visible Spectrophotometer) instrument at the wavelength of maximum absorbance of 664 nm.

3. Results and discussion

3.1. $BiVO_4$ catalysts characterization

3.1.1. XRD analysis

The effect of different synthesis conditions of temperature and pH values on the phase structure and morphology of $BiVO_4$ were characterized by XRD. At a synthesis pH of 7, it can be observed from Fig. 1A that the crystalline phase of all $BiVO_4$ samples can be well indexed according to monoclinic scheelite structure with the presence of weak peaks at 2θ = 15.5°, strong peaks at 2θ = 28.9° and the splitting of peaks at 2θ = 18.5°, 35°, and 47° (JCPDS no. 01-075-1867), corresponding with the XRD patterns of the study reported earlier (Zhao et al., 2016). Furthermore, the cell parameters of the $BiVO_4$ samples are presented in Table 1. As shown in Table 1, the crystallographic parameter of the $BiVO_4$ sample corresponds to the cell parameters of the monoclinic scheelite. Moreover, we observed that intensities of the major diffracted peaks changed remarkably under different synthesis conditions of temperature (Fig. 1A). A remarkable increase in the intensity ratio of $I_{(0\ 4\ 0)}/I_{(1\ 2\ 1)}$ from 0.2212 to 1.1846 was observed when the synthesis temperature increased from 80 to 140 °C, whereas the change of the intensity ratio of $I_{(0\ 1\ 1)}/I_{(1\ 2\ 1)}$ tended to be opposite (Table 1). However, with excessively

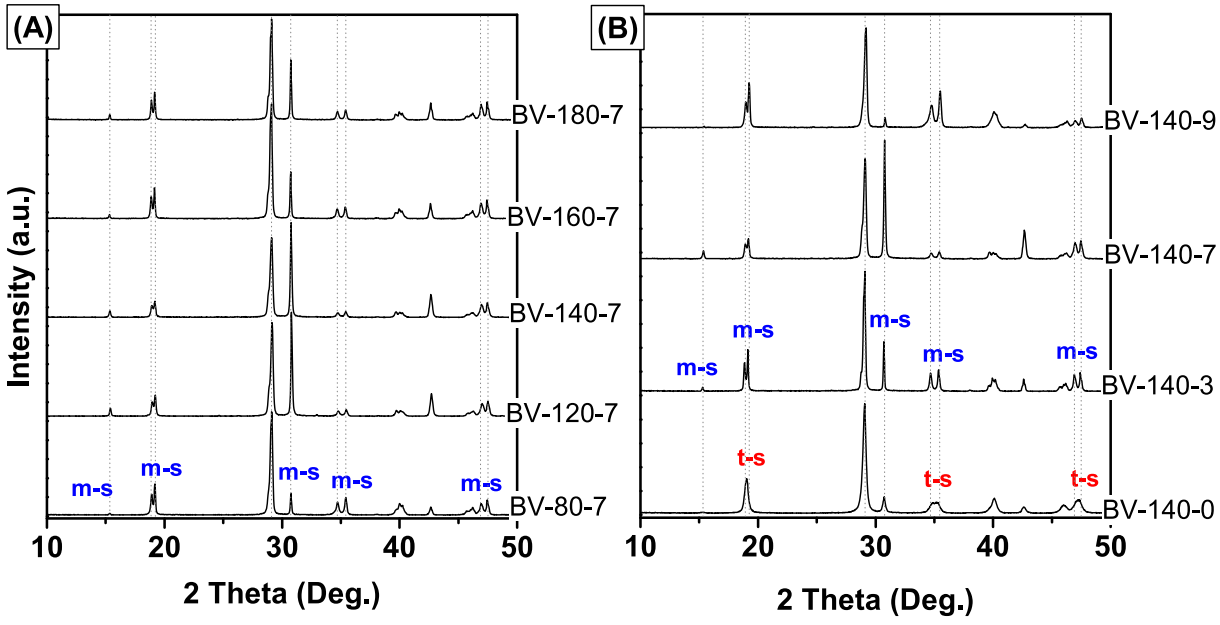

Fig. 1 XRD patterns of $BiVO_4$ synthesized at different temperatures (A) and pH (B).

Table 1 Lattice parameters for the $BiVO_4$ samples.

Sample codes	Synthesis conditions		Unit cell parameters					L_{XRD} (nm)	I_{040}/I_{121}	I_{011}/I_{121}
	Temperature (°C)	pH	a (Å)	b (Å)	c (Å)	β (Å)	V_{cell} (Å^3)			
BV-80-7	80	7	5.1653	11.6327	5.0672	90.4065	304.460	31.64	0.2212	0.3105
BV-120-7	120	7	5.1567	11.6111	5.0629	90.3403	303.1358	52.90	1.1102	0.2348
BV-140-7	140	7	5.1646	11.6283	5.0677	90.3876	304.3328	49.11	1.1846	0.2096
BV-160-7	160	7	5.1689	11.6402	5.0746	90.4005	305.3124	32.70	0.4188	0.2563
BV-180-7	180	7	5.1645	11.6337	5.0805	90.5537	305.2350	32.41	0.5959	0.2823
BV-140-0	140	0	5.1949	11.7342	5.0967	91.1195	310.6215	25.20	0.1594	0.3237
BV-140-3	140	3	5.1700	11.6497	5.0753	90.4569	305.6720	35.24	1.0561	0.6582
BV-140-9	140	9	5.1597	11.6078	5.0562	90.5965	302.8113	29.28	1.0551	0.6596

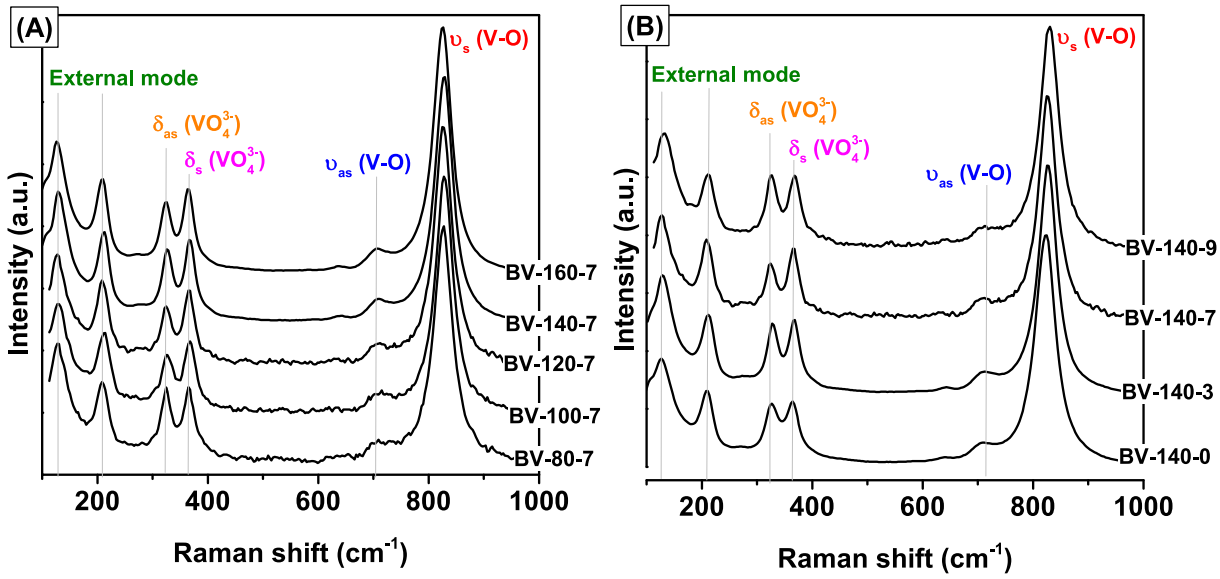

Fig. 2 Ramman spectra of $BiVO_4$ samples synthesized at different temperature (A) and pH (B).

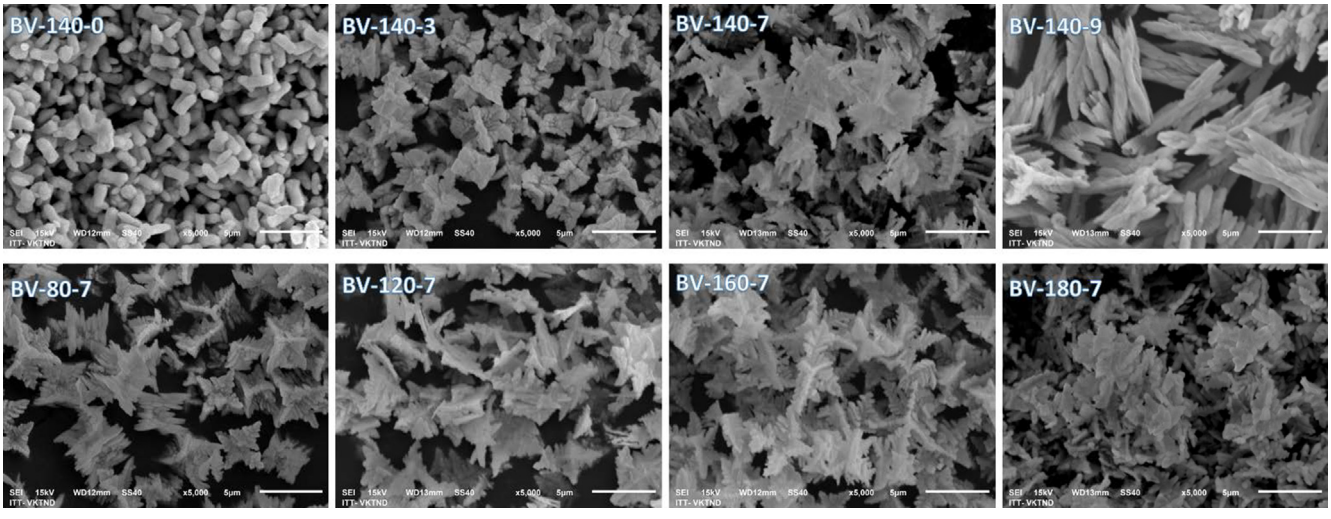

Fig.3 SEM images of $BiVO_4$ samples synthesized at different temperature (A) and pH (B).

high synthesis temperatures, the trend seemed to overturn. Especially, when the synthesis temperature was fixed at 140 °C, the intensity of (0 4 0) facets reaches the highest level while the intensity of (0 4 0) facets reaches the lowest level.

Regarding the effects of pH (Fig. 1B), the as-synthesized $BiVO_4$ samples exhibited a monoclinic scheelite structure when the pH of precursor solution was fixed as 3, 7, and 9, whereas the $BiVO_4$ with tetragonal scheelite phase was observed when the pH value was 0. The XRD analysis showed that different synthesis conditions of temperature and pH significantly affected the growth of $BiVO_4$ crystals oriented along (0 4 0) facets. These results are supported by results of previous studies, demonstrating that the growth of $BiVO_4$ crystals oriented along (0 4 0) facets will be beneficial to enhance the photocatalytic activity of monoclinic scheelite $BiVO_4$ (Tan et al., 2016).

3.1.2. Ramman analysis

Raman spectra of the $BiVO_4$ samples were presented in Fig. 2, which demonstrated that $BiVO_4$ was synthesized with a monoclinic crystalline structure. The monoclinic $BiVO_4$ sample has six vibration modes including the external vibration mode of $BiVO_4$ at 127 and 203 cm^{-1}, the asymmetric and symmetric deformation vibration mode of VO_4^{-3} groups at 324 cm^{-1} and 366 cm^{-1}, the asymmetric stretching vibration mode of V—O bonds at 644 and 709 cm^{-1}, and the symmetric stretching vibration mode of V—O bonds at 824 cm^{-1} (Phu et al., 2016). In addition, Raman signals corresponding to vanadium oxide or bismuth oxide was not observed in all samples. These results are in good agreement with the XRD results.

3.1.3. FESEM analysis

The crystal shape, particle size and particle distribution of the material were observed through SEM images. The crystal shape of the resulting material varies widely when the solvothermal process is conducted at different temperatures and pH values (Fig. 3). This result proved that the morphology of $BiVO_4$ is dependent on the solvothermal route. Especially, SEM images show that the synthesis pH has a significant influence on the crystal development process of materials. For samples synthesized at 140 °C, the crystal shape changed from a peanut-like to a rod when the synthesis pH increased from 0 to 9. At solvothermal pH of 7, it can be seen from Fig. 3 that the sample BV-140-7 shows a leaf-like structure. Furthermore, in this study, the SEM results indicate that different crystalline morphologies also relate to the temperature used for synthesis. With low temperatures corresponding to the low diffusion rate of crystal nuclei, crystal formation has a 3D structure and is relatively homogeneous. Meanwhile, the high synthetic temperature accelerates the diffusion rate of crystal nuclei, thus forming a leaf-like crystal with uneven size and heterogeneous morphology.

3.1.4. UV–vis DRS analysis

The light absorption properties of $BiVO_4$ samples were examined by UV–vis DRS. Fig. 4 shows the UV–vis DRS of as-prepared $BiVO_4$ samples, which were prepared using different synthesis conditions of temperature and pH. As shown in Fig. 4, all the $BiVO_4$ exhibited absorption-edge in the visible light range at about $\lambda = 535$ nm. According to the absorbance of visible light of $BiVO_4$ materials, the photocatalytic property was enhanced in the visible light region. The band-gap energy

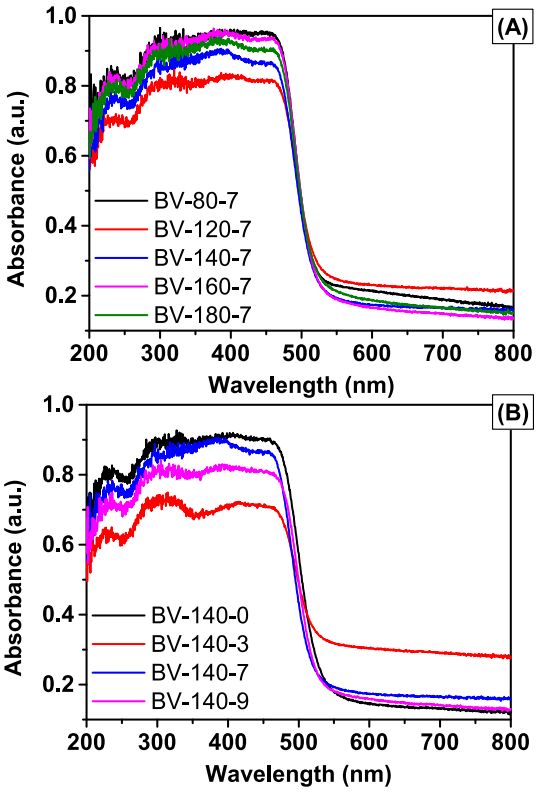

Fig. 4 UV–Vis DRS spectra of the $BiVO_4$ samples synthesized at different temperature (A) and pH (B).

(E_g) of all the $BiVO_4$ samples was calculated from the Tauc plot (Jo et al., 2015). The E_g value is presented in Table 2. As can be seen in Table 2, the E_g values are in the range from 2.29 to 2.41 eV, this result is consistent with E_g value of $BiVO_4$ with the monoclinic crystal structure (Kohtani et al., 2003).

3.2. Photocatalytic degradation of MB

The photocatalytic activities of as-synthesized $BiVO_4$ photocatalysts were evaluated by the photodegradation of methylene blue (MB) dye in water solution in the presence of LED light. We have found that by using appropriate synthesis conditions (including temperature and pH) the $BiVO_4$ exhibited high photocatalytic efficiency for MB degradation, as shown in Fig. 5. With different synthesis conditions of temperature, after visible light irradiation for 180 min, removal of MB was about 57.26%, 77.40%, 82.30%, 72.40%, and 73.80% in BV-80-7/visible light catalytic system, BV-120-7/visible light catalytic system, BV-140-7/visible light catalytic system, BV-160-7/visible light catalytic system, and BV-180-7/visible light catalytic system, respectively. From the obtained result, we observed that the BV-140–7 exhibited much higher activity than those of other samples and higher than that of previous studies (Chen et al., 2013; Zhao et al., 2018). In addition, the photocatalytic degradation of MB according to the first kinetics and the reaction rate constants of the samples are listed in Table 2. As shown in Table 2, the photodegradation rate constant (k) of BV-140–7 was higher than those of the other samples. Because of this synthetic condition the growth of $BiVO_4$ crystals oriented along (0 4 0) facets. It will be beneficial to

Table 2 The band-gap energy and the rate constant of the $BiVO_4$ samples.

Sample codes	E_g (eV)	k_{app} (10^{-3} min^{-1})	R^2
BV-80-7	2.34	4.62	0.9979
BV-120-7	2.40	7.30	0.9431
BV-140-7	2.33	7.94	0.9526
BV-160-7	2.29	5.91	0.9182
BV-180-7	2.41	6.58	0.9207
BV-140-0	2.30	5.69	0.9467
BV-140-3	2.37	7.70	0.9765
BV-140-9	2.38	5.00	0.9751

enhance the photocatalytic activity of monoclinic scheelite $BiVO_4$.

The change in the UV–vis absorption spectrum of CV over time in the presence of BV-140–7 is shown in Fig. 5C. As the irradiation duration was prolonged, the maximum absorption peak of MB at a wavelength of 664 nm decreased. Moreover, no increase in the absorption peak of MB in the UV region was found during irradiation, suggesting that most MB has completely decomposed without producing intermediate compounds.

The photocatalytic activities of as-synthesized $BiVO_4$ photocatalysts were evaluated by the photodegradation of methylene blue (MB) dye in water solution in the presence of LED light. We have found that by using appropriate synthesis conditions (including temperature and pH) the $BiVO_4$ exhibited high photocatalytic efficiency for MB degradation, as shown in Fig. 5. With different synthesis conditions of temperature, after visible light irradiation for 180 min, removal of MB was about 57.26%, 77.40%, 82.30%, 72.40%, and 73.80% in BV-80-7/light catalytic system, BV-120-7/light catalytic system, BV-140-7/light catalytic system, BV-160-7/light catalytic system, and BV-180-7/light catalytic system, respectively. From the obtained result, we observed that the BV-140-7 exhibited much higher activity than those of other samples. In addition, the photocatalytic degradation of MB according to the first kinetics and the reaction rate constants (k) of the samples are listed in Table 2. As shown in Table 2, the k value of BV-140-7 was higher than those of the other samples. This result could be explained as a consequence of the appropriate morphology under this synthetic condition.

Mechanism of photodegradation organic compounds using monoclinic scheelite $BiVO_4$ crystals oriented along (0 4 0) facets was suggested in Fig. 6. Firstly, monoclinic scheelite $BiVO_4$ crystals oriented along (0 4 0) facets are excited to generate the photoexcited electrons (e^-) and the positive holes (h^+) under the white LED light irradiation. Then, e^- and h^+ are transferred to the catalyst surface and reacted with O_2 and H_2O to yield $^{-}\cdot O_2$ and $OH^{\cdot}$, respectively. e^- and h^+ tend to move towards (0 1 0) and (1 1 0) faces, leading to oxidation and reduction reactions that occur on {0 1 0} and (1 1 0) faces, respectively.(Tan et al., 2016) Finally, the MB molecules were oxidized by radicals such as $OH^{\cdot}$ and/or h^+.

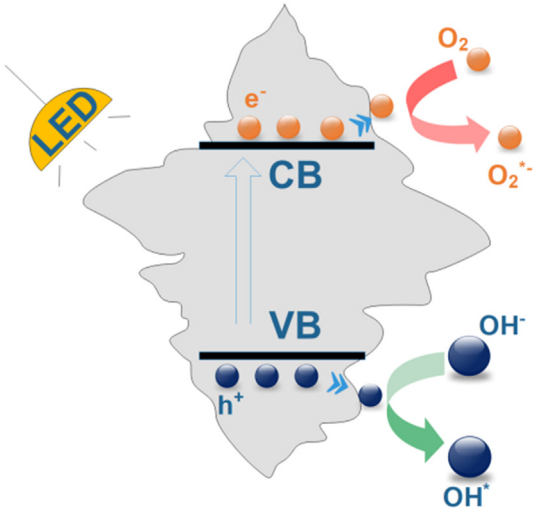

Fig. 6 Mechanism of photodegradation organic compounds using monoclinic scheelite $BiVO_4$ crystals oriented along (0 4 0) facets.

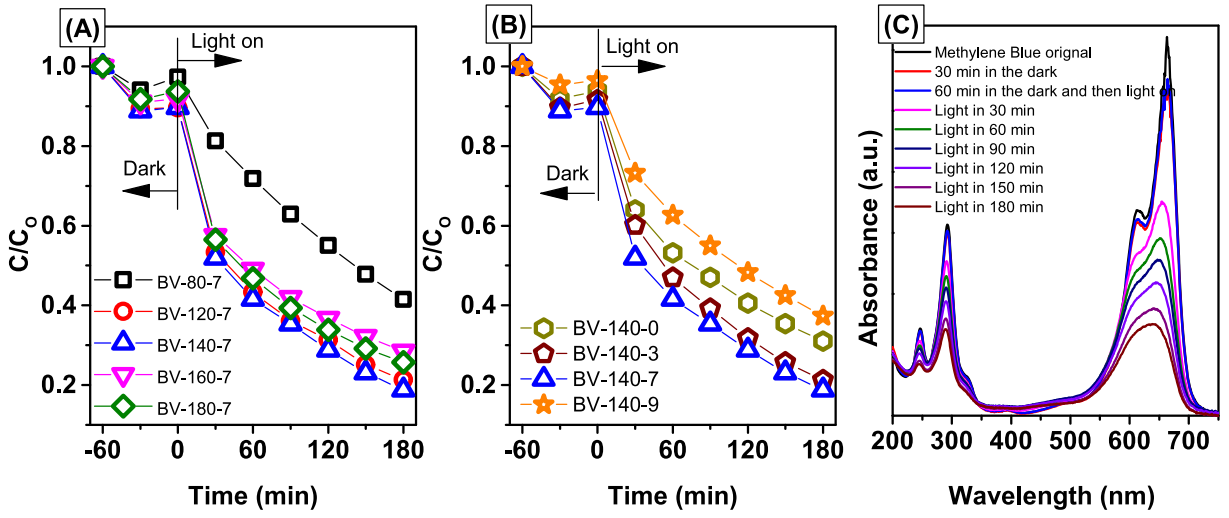

Fig. 5 Photocatalytic degradation of MB over $BiVO_4$ samples synthesized at difference temperature (A) and pH (B), and UV–vis absorption spectra (C) of MB solutions during illumination using BV-140-7 sample.

4. Conclusion

The monoclinic scheelite $BiVO_4$ photocatalytic material with the high photocatalytic degradation efficiency of MB was successfully synthesized by a solvothermal process using a solvent mixture of ethylene glycol and water. The results indicate that the synthesis temperatures and pH exerted a strong influence on the morphology and crystal facet of $BiVO_4$. The crystal facets were significantly affected by the separation of electron and hole pairs during the reaction process. In this study, the as-prepared $BiVO_4$ with crystal facets ratio of (0 4 0)/(1 2 1) of 1.1846 (BV-140-7 sample) exhibited the high degradation of MB, in which 82.30% removal of MB was achieved within 180 min.

Declaration of Competing Interest

The authors declare that they have no known competing financial interests or personal relationships that could have appeared to influence the work reported in this paper.

Acknowledgments

This research is funded by Vietnam National Foundation for Science and Technology Development (NAFOSTED) under grant number 104.05-2017.315.

References

Abbasi, M., Rafique, U., Murtaza, G., Ashraf, M.A., 2018. Synthesis, characterisation and photocatalytic performance of ZnS coupled Ag2S nanoparticles: A remediation model for environmental pollutants. Arab. J. Chem. 11, 827–837. https://doi.org/10.1016/j.arabjc.2017.12.017.

Abdennouri, M., Baâlala, M., Galadi, A., El Makhfouk, M., Bensitel, M., Nohair, K., Sadiq, M., Boussaoud, A., Barka, N., 2016. Photocatalytic degradation of pesticides by titanium dioxide and titanium pillared purified clays. Arab. J. Chem. 9, S313–S318. https://doi.org/10.1016/j.arabjc.2011.04.005.

Ameta, Rakshit, Ameta, S.C., 2016. Photocatalysis: Principles and Applications. CRC Press, Boca Raton. https://doi.org/10.1201/9781315372396.

Chen, L., Huang, R., Ma, Y.-J., Luo, S.-L., Au, C.-T., Yin, S.-F., 2013. Controllable synthesis of hollow and porous Ag/BiVO4 composites with enhanced visible-light photocatalytic performance. RSC Adv. 3, 24354–24361. https://doi.org/10.1039/C3RA43691H.

Chen, L., Wang, J., Meng, D., Xing, Y., Tian, X., Yu, X., Xu, K., Wu, X., 2015. Effects of citric acid and urea on the structural and morphological characteristics of BiVO4 synthesized by the sol–gel combustion method. J. Sol-Gel Sci. Technol. 76, 562–571. https://doi.org/10.1007/s10971-015-3806-1.

Jo, W.J., Kang, H.J., Kong, K.-J., Lee, Y.S., Park, H., Lee, Y., Buonassisi, T., Gleason, K.K., Lee, J.S., 2015. Phase transition-induced band edge engineering of BiVO4 to split pure water under visible light. Proc. Natl. Acad. Sci. U. S. A. 112, 13774–13778. https://doi.org/10.1073/pnas.1509674112.

Kohtani, S., Koshiko, M., Kudo, A., Tokumura, K., Ishigaki, Y., Toriba, A., Hayakawa, K., Nakagaki, R., 2003. Photodegradation of 4-alkylphenols using BiVO4 photocatalyst under irradiation with visible light from a solar simulator. Appl. Catal. B Environ. 46, 573–586. https://doi.org/10.1016/S0926-3373(03)00320-5.

Lim, A.R., Choh, S.H., Jang, M.S., 1995. Prominent ferroelastic domain walls in BiVO4crystal. J. Phys. Condens. Matter. 7, 7309–7323. https://doi.org/10.1088/0953-8984/7/37/005.

Liu, W., Cao, L., Su, G., Liu, H., Wang, X., Zhang, L., 2010. Ultrasound assisted synthesis of monoclinic structured spindle BiVO4 particles with hollow structure and its photocatalytic property. Ultrason. Sonochem. 17, 669–674. https://doi.org/10.1016/j.ultsonch.2009.12.012.

Martínez-de la Cruz, A., Pérez, U.M.G., 2010. Photocatalytic properties of BiVO4 prepared by the co-precipitation method: Degradation of rhodamine B and possible reaction mechanisms under visible irradiation. Mater. Res. Bull. 45, 135–141. https://doi.org/10.1016/j.materresbull.2009.09.029.

Phu, N.D., Hoang, L.H., Vu, P.K., Kong, M.-H., Chen, X.-B., Wen, H.C., Chou, W.C., 2016. Control of crystal phase of BiVO4 nanoparticles synthesized by microwave assisted method. J. Mater. Sci. Mater. Electron. 27, 6452–6456. https://doi.org/10.1007/s10854-016-4585-3.

Rajamanickam, D., Shanthi, M., 2016. Photocatalytic degradation of an organic pollutant by zinc oxide – solar process. Arab. J. Chem. 9, S1858–S1868. https://doi.org/10.1016/j.arabjc.2012.05.006.

Ressnig, D., Kontic, R., Patzke, G.R., 2012. Morphology control of BiVO4 photocatalysts: pH optimization vs. self-organization. Mater. Chem. Phys. 135, 457–466. https://doi.org/10.1016/j.matchemphys.2012.05.008.

Singh, P., Shandilya, P., Raizada, P., Sudhaik, A., Rahmani-Sani, A., Hosseini-Bandegharaei, A., 2020. Review on various strategies for enhancing photocatalytic activity of graphene based nanocomposites for water purification. Arab. J. Chem. 13, 3498–3520. https://doi.org/10.1016/j.arabjc.2018.12.001.

Sun, Y., Wu, C., Long, R., Cui, Y., Zhang, S., Xie, Y., 2009. Synthetic loosely packed monoclinic BiVO4 nanoellipsoids with novel multiresponses to visible light, trace gas and temperature. Chem. Commun., 4542–4544 https://doi.org/10.1039/B907406F.

Tan, H.L., Wen, X., Amal, R., Ng, Y.H., 2016. BiVO4 010 and 110 relative exposure extent: governing factor of surface charge population and photocatalytic activity. J. Phys. Chem. Lett. 7, 1400–1405. https://doi.org/10.1021/acs.jpclett.6b00428.

Xi, G., Ye, J., 2010. Synthesis of bismuth vanadate nanoplates with exposed 001 facets and enhanced visible-light photocatalytic properties. Chem. Commun. 46, 1893–1895. https://doi.org/10.1039/B923435G.

Zhao, Z., Dai, H., Deng, J., Liu, Y., Au, C.T., 2013. Effect of sulfur doping on the photocatalytic performance of BiVO4 under visible light illumination. Chin. J. Catal. 34, 1617–1626. https://doi.org/10.1016/S1872-2067(12)60632-9.

Zhao, G., Liu, W., Li, J., Lv, Q., Li, W., Liang, L., 2016. Facile synthesis of hierarchically structured BiVO4 oriented along (010) facets with different morphologies and their photocatalytic properties. Appl. Surf. Sci. 390, 531–539. https://doi.org/10.1016/j.apsusc.2016.08.126.

Zhao, G., Liu, W., Hao, Y., Zhang, Z., Li, Q., Zang, S., 2018. Nanostructured shuriken-like BiVO4 with preferentially exposed 010 facets: preparation, formation mechanism, and enhanced photocatalytic performance. Dalt. Trans. 47, 1325–1336. https://doi.org/10.1039/C7DT04431C.